

Pressure and Phase Equilibria in Interacting Active Brownian Spheres

Alexandre P. Solon,¹ Joakim Stenhammar,² Raphael Wittkowski,²
Mehran Kardar,³ Yariv Kafri,⁴ Michael E. Cates,² and Julien Tailleur¹

¹*Laboratoire, Matière et Systèmes Complexes, UMR 7057 CNRS/P7,
Université Paris Diderot, 75205 Paris Cedex 13, France*

²*SUPA, School of Physics and Astronomy, University of Edinburgh, Edinburgh EH9 3FD, United Kingdom*

³*Massachusetts Institute of Technology, Department of Physics, Cambridge, Massachusetts 02139, USA*

⁴*Department of Physics, Technion, Haifa 32000, Israel*

(Dated: June 16, 2015)

We derive a microscopic expression for the mechanical pressure P in a system of spherical active Brownian particles at density ρ . Our exact result relates P , defined as the force per unit area on a bounding wall, to bulk correlation functions evaluated far away from the wall. It shows that (i) $P(\rho)$ is a state function, independent of the particle-wall interaction; (ii) interactions contribute two terms to P , one encoding the slow-down that drives motility-induced phase separation, and the other a direct contribution well known for passive systems; (iii) P is equal in coexisting phases. We discuss the consequences of these results for the motility-induced phase separation of active Brownian particles, and show that the densities at coexistence *do not* satisfy a Maxwell construction on P .

PACS numbers: 05.40.-a; 05.70.Ce; 82.70.Dd; 87.18.Gh

Much recent research addresses the statistical physics of active matter, whose constituent particles show autonomous dissipative motion (typically self-propulsion), sustained by an energy supply. Progress has been made in understanding spontaneous flow [1] and phase equilibria in active matter [4–7], but as yet there is no clear thermodynamic framework for these systems. Even the definition of basic thermodynamic variables such as temperature and pressure is problematic. While “effective temperature” is a widely used concept outside equilibrium [7], the discussion of pressure, P , in active matter has been neglected until recently [8–10, 12–14]. At first sight, because P can be defined mechanically as the force per unit area on a confining wall, its computation as a statistical average looks unproblematic. Remarkably though, it was recently shown that for active matter the force on a wall can depend on details of the wall-particle interaction so that P is not, in general, a state function [15].

Active particles are nonetheless clearly capable of exerting a mechanical pressure P on their containers. (When immersed in a space-filling solvent, this becomes an *osmotic* pressure [8, 10].) Less clear is how to calculate P ; several suggestions have been made [8–10, 12] whose inter-relations are, as yet, uncertain. Recall that for systems in thermal equilibrium, the mechanical and thermodynamic definitions of pressure (force per unit area on a confining wall, and $-(\partial\mathcal{F}/\partial V)_N$ for N particles in volume V , with \mathcal{F} the Helmholtz free energy) necessarily coincide. Accordingly, various formulae for P (involving, e.g., the density distribution near a wall [16], or correlators in the bulk [5, 17]) are always equivalent. This ceases to be true, in general, for active particles [8, 15].

In this Letter we adopt the mechanical definition of P . We first show analytically that P is a state function, independent of the wall-particle interaction, for one important and well-studied class of systems: spherical active

Brownian particles (ABPs) with isotropic repulsions. By definition, such ABPs undergo overdamped motion in response to a force that combines an arbitrary pair interaction with an external forcing term of constant magnitude along a body axis; this axis rotates by angular diffusion. While not a perfect representation of experiments (particularly in bulk fluids, where self-propulsion is created internally and hydrodynamic torques arise [19]), ABPs have become the mainstay of recent simulation and theoretical studies [5–7, 20–24]. They provide a benchmark for the statistical physics of active matter, and a simplified model for the experimental many-body dynamics of autophoretic colloidal swimmers, or other active systems, coupled to a momentum reservoir such as a supporting surface [24–29]. (We comment below on the momentum-conserving case.) By generating large amounts of data in systems whose dynamics and interactions are precisely known, ABP simulations are currently better placed than experiments to answer fundamental issues concerning the physics of active pressure, such as those raised in [9, 10].

Our key result exactly relates P to bulk correlators, powerfully generalizing familiar results for the passive case. The pressure for ABPs is the sum of an ideal-gas contribution and a non-ideal one stemming from interactions. Crucially, the latter results from *two* contributions: one is a standard, ‘direct’ term (the density of pairwise forces acting across a plane), which we call P_D , while the other, ‘indirect’ term, absent in the passive case, describes the reduction in momentum flux caused by collisional slowdown of the particles. For short-ranged repulsions and high propulsive force, P_D becomes important only at high densities; the indirect term dominates at intermediate densities and is responsible for motility-induced phase separation (MIPS) [4, 6, 7]. The same calculation establishes that, for spherical ABPs (though not in general [15]) P must be equal in all coexisting phases.

We further show that our ideal and indirect terms together form exactly the ‘swim pressure’, $P_S(\rho)$ at density ρ , previously defined via a force-moment integral in [9, 10], and moreover that (in 2D) P_S is simply $\rho v(0)v(\rho)/(2D_r)$, where $v(\rho)$ is the mean propulsive speed of ABPs and D_r their rotational diffusivity. We interpret this result, and show that (for $P_D = 0$) the mechanical instability, $dP_S/d\rho = 0$, coincides exactly with a diffusive one previously found to cause MIPS among particles whose interaction comprises a density-dependent swim speed $v(\rho)$ [4, 6, 7]. We briefly explain why this correspondence does not extend to phase equilibria more generally, deferring a full account to a longer paper [1].

To calculate the pressure in interacting ABPs, we follow [15] and consider the dynamics in the presence of an explicit, conservative wall-particle force \mathbf{F}_w . For simplicity, we work in 2D, and consider periodic boundary conditions in y and confining walls parallel to $\mathbf{e}_y = (0, 1)$. We start from the standard Langevin dynamics of ABPs with bare speed v_0 , interparticle forces \mathbf{F} and unit mobility [5, 6, 34]:

$$\begin{aligned}\dot{\mathbf{r}}_i &= v_0 \mathbf{u}(\theta_i) + F_w(x_i) \mathbf{e}_x + \sum_{j \neq i} \mathbf{F}(\mathbf{r}_j - \mathbf{r}_i) + \sqrt{2D_t} \boldsymbol{\eta}_i, \\ \dot{\theta}_i &= \sqrt{2D_r} \xi_i.\end{aligned}\quad (1)$$

Here $\mathbf{r}_i(t) = (x_i, y_i)$ is the position, and $\theta_i(t)$ the orientation, of particle i at time t ; $\mathbf{u}(\theta) = (\cos(\theta), \sin(\theta))$; $F_w = \|\mathbf{F}_w\|$ is a force acting along the wall normal $\mathbf{e}_x = (1, 0)$; D_t is the bare translational diffusivity; and $\boldsymbol{\eta}_i(t)$ and $\xi_i(t)$ are zero-mean unit-variance Gaussian white noises with no correlations among particles.

Following standard procedures [6, 7, 35, 36] this leads to an equation for the fluctuating distribution function $\hat{\psi}(\mathbf{r}, \theta, t)$ whose zeroth, first, and second angular harmonics are the fluctuating particle density $\hat{\rho} = \int \hat{\psi} d\theta$; the x -polarization $\hat{\mathcal{P}} = \int \hat{\psi} \cos(\theta) d\theta$; and $\hat{\mathcal{Q}} = \int \hat{\psi} \cos(2\theta) d\theta$, which encodes nematic order normal to the wall:

$$\begin{aligned}\dot{\hat{\psi}} &= -\nabla \cdot \left((v_0 \mathbf{u}(\theta) + F_w(x) \mathbf{e}_x + \int \mathbf{F}(\mathbf{r}' - \mathbf{r}) \hat{\rho}(\mathbf{r}') d^2 r') \hat{\psi} \right) \\ &+ D_r \partial_\theta^2 \hat{\psi} + D_t \nabla^2 \hat{\psi} + \nabla \cdot (\sqrt{2D_t} \hat{\psi} \boldsymbol{\eta}) + \partial_\theta (\sqrt{2D_r} \hat{\psi} \xi),\end{aligned}\quad (2)$$

where $\boldsymbol{\eta}(\mathbf{r}, t)$ and $\xi(\mathbf{r}, t)$ are δ -correlated, zero-mean, and unit-variance, Gaussian white noise fields. In steady-state, the noise-averages $\rho = \langle \hat{\rho} \rangle$, $\mathcal{P} = \langle \hat{\mathcal{P}} \rangle$, and $\mathcal{Q} = \langle \hat{\mathcal{Q}} \rangle$ are, by translational invariance, functions of x only, as is the wall force $F_w(x)$ [37]. Integrating (2) over θ , and then averaging over noise in steady state gives $\partial_x J = 0$, with J the particle current. For any system with impermeable boundaries, $J = 0$. Writing this out explicitly gives:

$$0 = v_0 \mathcal{P} + F_w \rho - D_t \partial_x \rho + I_1(x), \quad (3)$$

$$I_1(x) \equiv \int F_x(\mathbf{r}' - \mathbf{r}) \langle \hat{\rho}(\mathbf{r}') \hat{\rho}(\mathbf{r}) \rangle d^2 r'. \quad (4)$$

Applying the same procedure to the first angular har-

monic gives

$$D_r \mathcal{P} = -\partial_x \left[\frac{v_0}{2} (\rho + \mathcal{Q}) + F_w \mathcal{P} - D_t \partial_x \mathcal{P} + I_2(x) \right], \quad (5)$$

$$I_2(x) \equiv \int F_x(\mathbf{r}' - \mathbf{r}) \langle \hat{\rho}(\mathbf{r}') \hat{\mathcal{P}}(\mathbf{r}) \rangle d^2 r'. \quad (6)$$

Note that the integrals I_1 and I_2 defined in (4) and (17) are, by translational invariance, functions only of x .

The mechanical pressure on the wall is the spatial integral of the force density exerted upon it by the particles. The wall force obeys $F_w = -\partial_x U_w$ where an origin is chosen so that U_w is non-zero only for $x > 0$. The wall is confining, i.e. $F_w \rho \rightarrow 0$ for $x \gg 0$, whereas $x = \Lambda \ll 0$ denotes any plane in the bulk of the fluid, far from the wall. By Newton’s third law, the pressure is then

$$P = - \int_\Lambda^\infty F_w(x) \rho(x) dx, \quad (7)$$

In (19) we now use (3) to set $-F_w \rho = v_0 \mathcal{P} - D_t \partial_x \rho + I_1$:

$$P = v_0 \int_\Lambda^\infty \mathcal{P}(x) dx + D_t \rho(\Lambda) + \int_\Lambda^\infty I_1(x) dx. \quad (8)$$

We next use (5), in which \mathcal{P} and \mathcal{Q} vanish in the bulk and all terms vanish at infinity, to evaluate $\int \mathcal{P} dx$, giving:

$$P = \frac{v_0}{D_r} \left(\frac{v_0}{2} \rho(\Lambda) + I_2(\Lambda) \right) + D_t \rho(\Lambda) + \int_\Lambda^\infty I_1(x) dx. \quad (9)$$

Using Newton’s third law, the final integral in (9) takes a familiar form, describing the density of pair forces acting across some plane through the bulk (far from any wall):

$$\int_{x > \Lambda} dx \int_{x' < \Lambda} d^2 r' F_x(\mathbf{r}' - \mathbf{r}) \langle \hat{\rho}(\mathbf{r}') \hat{\rho}(\mathbf{r}) \rangle \equiv P_D. \quad (10)$$

Thus in the passive limit ($v_0 = 0$) we recover in P_D the standard interaction part in the pressure [5]. We call P_D the ‘‘direct’’ contribution; it is affected by activity only through changes to the correlator. Activity also enters (via v_0) the well-known ideal pressure term [9, 10, 13, 15]:

$$P_0 \equiv \left(D_t + \frac{v_0^2}{2D_r} \right) \rho(\Lambda). \quad (11)$$

Having set friction to unity in (1), $D_t = k_B T$, so that within P_0 (only) activity looks like a temperature shift.

Most strikingly, activity in combination with interactions also brings an ‘‘indirect’’ pressure contribution

$$P_1 \equiv \frac{v_0}{D_r} I_2(\Lambda) \quad (12)$$

with no passive counterpart. Here $I_2(\Lambda)$ is again a wall-independent quantity, evaluated on *any* bulk plane $x = \Lambda \ll 0$. We discuss this term further below.

Our exact result for mechanical pressure is finally

$$P = P_0 + P_1 + P_D \quad (13)$$

with these three terms defined by (11), (12), and (10), respectively. P is thus for interacting ABPs a state function, calculable solely from bulk correlations and independent of the particle-wall force $F_w(x)$. Because the same boundary force can be calculated using *any* bulk plane $x = \Lambda$, it follows that, should the system undergo phase separation, P is the same in all coexisting phases [37]. This proves for ABPs an assumption that, while plausible [10, 38], is not obvious, and indeed can fail for particles interacting via a density-dependent swim speed rather than direct interparticle forces [15].

Notably, although ABPs exchange momentum with a reservoir, (1) also describes particles swimming through a momentum-conserving bulk fluid, in an approximation where inter-particle and particle-wall hydrodynamic interactions are both neglected. So long as the wall interacts *solely* with the swimmers, our results above continue to apply to what is now the *osmotic* pressure.

The physics of the indirect contribution P_1 is that interactions between ABPs reduce their motility as the density increases. The ideal pressure term P_0 normally represents the flux of momentum through a bulk plane carried by particles that *move* across it (as opposed to those that *interact* across it) [17]. In our overdamped system one should replace in the preceding sentence ‘momentum’ with ‘propulsive force’ (plus a random force associated with D_t). Per particle, the propulsive force is density-independent, but the rate of crossing the plane is not. Accordingly we expect the factor v_0^2 in (11) to be modified by interactions, with one factor v_0 (force or momentum) unaltered, but the other (speed) replaced by a density-dependent contribution $v(\rho) \leq v_0$:

$$P_0 + P_1 = \left(D_t + \frac{v_0 v(\rho)}{2D_r} \right) \rho. \quad (14)$$

This requires the mean particle speed to obey

$$v(\rho) = v_0 + 2I_2/\rho. \quad (15)$$

Remarkably, (14) and (15) are *exact* results, where (15) is found from the mean speed of particle i in bulk, $v = v_0 + \langle \mathbf{u}(\theta_i) \cdot \sum_{j \neq i} \mathbf{F}(\mathbf{r}_j - \mathbf{r}_i) \rangle$. To see why this average involves I_2 , note that the system is isotropic in bulk, so x and y can be interchanged in $I_2(x)$, and that $\cos(\theta) \equiv \mathbf{u} \cdot \mathbf{e}_x$. Relation (17) then links v to I_2 via the $\langle \hat{\rho} \hat{\mathcal{P}} \rangle$ correlator, which describes the imbalance of forces acting on an ABP from neighbors in front and behind.

Furthermore, the self-propulsive term in (14) is exactly the ‘swim pressure’ P_S of [9, 10]:

$$\frac{v_0 v(\rho)}{2D_r} \rho = P_S \equiv \frac{\rho}{2} \langle \mathbf{r} \cdot \mathbf{F}^a \rangle \quad (16)$$

with $\mathbf{F}^a = v_0 \mathbf{u}$ a particle’s propulsive force and \mathbf{r} its position. (The particle mobility $v_0/F^a = 1$ in our units.) The equivalence of (12), (14), and (16) is proven analytically in [39] and confirmed numerically in Fig. 1 for ABP simulations performed as in [20, 21].

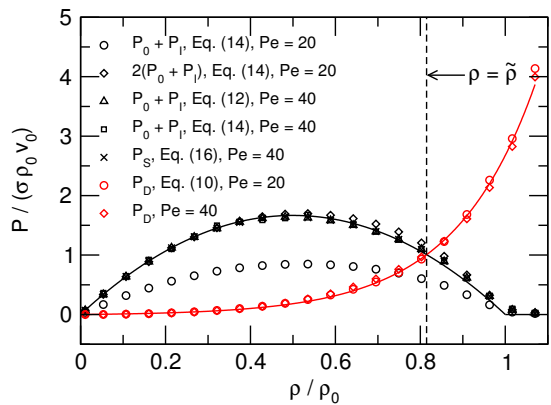


Figure 1. Numerical measurements of $P_0 + P_1$, P_S , and P_D in single-phase ABP simulations at Péclet number $Pe \equiv 3v_0/(D_r\sigma) = 40$, where σ is the particle diameter. Expressions (12), (14), and (16) for $P_0 + P_1$ and P_S show perfect agreement. Also shown is data for $Pe = 20$, unscaled and rescaled by factor 2. This confirms that $P_S = P_0 + P_1$ is almost linear in Pe ; small deviations arise from Pe -dependence of the correlators. In red is P_D for $Pe = 20, 40$, with no rescaling. Pe was varied using D_r , at fixed v_0 and with $D_t = D_r\sigma^2/3$. Solid lines are fits to piecewise parabolic (P_S) and exponential (P_D) functions used in the semi-empirical equation of state. ρ_0 is a near-close-packed density at which $v(\rho)$ vanishes and $\tilde{\rho}$ is the threshold density above which $P_D > P_S$. See [39] for details.

Thus for $D_t = 0$, (13) may alternatively be rewritten as $P = P_S + P_D$ [9, 10]. Together, our results confirm that P_S , defined in bulk via (16), determines (with P_D) the force acting on a confining wall. This was checked numerically in [9] but is not automatic [15]. Moreover, our work gives via (14) an exact kinetic expression for P_S with a clear and simple physical interpretation in terms of the transport of propulsive forces. This illuminates the nature of the swim pressure P_S and extends to finite ρ the limiting result $P_S = P_0$ [9, 10].

The connections made above are our central findings; they extend statistical thermodynamics concepts from equilibrium far into ABP physics. Before concluding, we ask how far these ideas extend to phase equilibria.

In the following we ignore for simplicity the D_t term (negligible in most cases [5, 7, 20, 34]). Then, assuming short-range repulsions, we have $P_S = \rho v_0 v(\rho)/(2D_r)$, with $v(\rho) \simeq v_0(1 - \rho/\rho_0)$ and ρ_0 a near-close-packed density [5, 6, 20]. P_D should scale as $\sigma \rho v_0 \mathcal{S}(\rho/\rho_0)$, where σ is the particle diameter and the function \mathcal{S} diverges at close packing; here the factor v_0 is because propulsive forces oppose repulsive ones, setting their scale [10]. Figure 1 shows that both the approximate expression for P_S (with a fitted $\rho_0 \simeq 1.19$ roughly independent of Pe), and the scaling of P_D , hold remarkably well. Defining a threshold value $\tilde{\rho}$ by $P_S(\tilde{\rho}) = P_D(\tilde{\rho})$ (see Fig. 1), it follows that at large enough Péclet number, $Pe = 3v_0/(D_r\sigma)$, P_S dominates completely for $\rho < \tilde{\rho}$, with P_D serving *only* to prevent the density from moving above the $\tilde{\rho}$ cutoff.

When $\rho < \tilde{\rho}$, P_D is negligible; the criterion $P'_S(\rho) < 0$, used in [10, 38] to identify a mechanical instability, is then via (16) *identical* to the spinodal criterion $(\rho v)' < 0$ used to predict MIPS in systems whose sole physics is a density-dependent speed $v(\rho)$ [6, 7]. Thus, for ABPs at large Pe , the mechanical theory reproduces one result of a long-established mapping between MIPS and equilibrium colloids with attractive forces [6, 7].

We next address the binodal densities of coexisting phases. According to [6, 7], particles with speed $v(\rho)$ admit an effective bulk free-energy density $f(\rho) = k_B T [\rho(\ln \rho - 1) + \int_0^\rho \ln v(u) du]$. (Interestingly, the equality of P in coexisting phases is equivalent at high Pe and $\rho < \tilde{\rho}$ to the equality of $k_B T \log(\rho v)$, which is the chemical potential in this ‘thermodynamic’ theory [4, 6].) The binodals are then found using a common tangent construction (CTC, i.e., global minimization) on f , or equivalently an equal-area Maxwell construction (MC) on an effective *thermodynamic* pressure $P_f = \rho f' - f$, which differs from P [8]. Formally, f is a local approximation to a large-deviation functional [40], whose nonlocal terms can (in contrast to equilibrium systems) alter the CTC or MC [8, 20]; we return to this issue below.

An appealing alternative is to apply the MC to the mechanical pressure P itself; this was, in different language, proposed in [38]. (The equivalence will be detailed in [1].) It amounts to constructing an effective free-energy density $f_P(\rho) \neq f$, defined via $P = \rho f'_P - f_P$, and using the CTC on f_P . However, f_P has no clear link to any large deviation functional [40]; and since it differs from f , these approaches *generically predict different binodals*.

To confirm this, we turn to the large Pe limit; here, for ABPs with $v(\rho) = v_0(1 - \rho/\rho_0)$ and $\tilde{\rho} = \rho_0$, we can explicitly construct $f(\rho)$ (and hence $P_f(\rho)$) alongside $P(\rho)$ (and hence $f_P(\rho)$), using our hard-cutoff approximation (i.e., a constraint $\rho < \tilde{\rho}$). All four functions are plotted in [39]; the two distinct routes indeed predict different binodals at high Pe (see Fig. 2) [42]. Each approach suffers its own limitations. That via f (or P_f) appears more accurate, but neglects non-local terms that can alter the binodals: although $f'(\rho)$ remains equal in coexisting phases, P_f is not equal once those terms are included [8]. The most serious drawback of this approach, currently, is that it cannot address finite Pe , where P_D no longer creates a sharp cutoff. Meanwhile the ‘mechanical’ route captures the equality of P in coexisting phases but unjustifiably assumes the MC on P , asserting in effect that f_P , and not f , is the effective free energy [40]. Nonlocal corrections [9] are again neglected.

At finite Pe where the crossover at $\tilde{\rho}$ is soft, (13) shows how P_I and P_D compete, giving Pe -dependent binodals (see Fig. 2). To test the predictions of the mechanical approach (equivalent to [38]), we set $P_D = \sigma \rho v_0 \mathcal{S}(\rho/\rho_0)$ as above, finding the function \mathcal{S} by numerics on single-phase systems at modest Pe (see Fig. 1). Adding this to P_S (assuming $P_S \propto Pe$ scaling) gives $P = P(\rho, Pe)$. At each Pe the binodal pressures and densities do lie on this equation of state, validating its semi-empirical

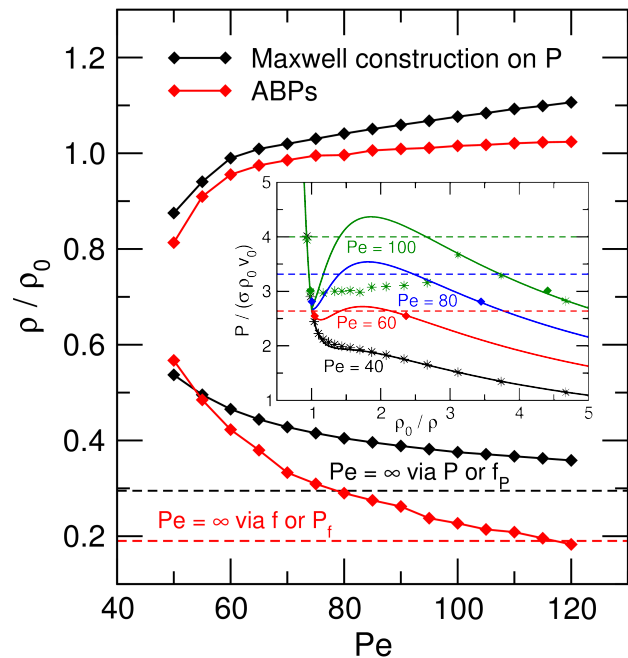


Figure 2. Simulated coexistence curves (binodals) for ABPs (red), and those calculated via the Maxwell construction (black) on the mechanical pressure P using the semi-empirical equation of state for P_S and P_D fitted from Fig. 1. Dashed lines: predicted high Pe asymptotes for the binodals calculated via f or P_f (lower), and calculated via P or f_P (upper). Inset: measured binodal pressures and densities (diamonds) fall on the equation-of-state curves but do not match the MC values (horizontal dashed lines). Stars show the $P(\rho)$ relation across the full density range from simulations at $Pe = 40$ and $Pe = 100$. The latter includes two metastable states at low density (high ρ_0/ρ) that are yet to phase separate.

form; but they do not obey the Maxwell construction on P , which must therefore be rejected (see Fig. 2, inset). We conclude that, despite our work and that of [38], no complete theory of phase equilibria in ABPs yet exists.

In summary, we have given in (10)-(13) an exact expression for the mechanical pressure P of active Brownian spheres. This relates P directly to bulk correlation functions and shows it to be a state function, independent of the wall interaction, something not true for all active systems [15]. As well as an ideal term P_0 , and a direct interaction term P_D , there is an indirect term P_I caused by collisional slowing down of propulsion. We established an exact link between $P_0 + P_I$ and the so called ‘swim pressure’ [10], allowing a clearer interpretation of that quantity. We showed that when MIPS arises in the regime of high $Pe = 3v_0/(D_r\sigma)$, the mechanical ($P' < 0$ [10]) and diffusive ($f'' < 0$ [6, 7]) instabilities coincide. That equivalence does not extend to the calculation of coexistence curves, for reasons we have explained. For simplicity we have worked in 2D; generalization of our results to 3D is straightforward [1] but notationally cumbersome.

The established description of MIPS as a diffusive in-

stability [6–8, 20] is fully appropriate in systems whose particles are ‘programmed’ to change their dynamics at high density (e.g., via bacterial quorum sensing [44, 45]), but it is not yet clear whether the same theory, or one based primarily on the mechanical pressure P , is better founded for finite-Pe phase equilibria in ABPs whose slowdown is collisional. Meanwhile, our exact results for P in these systems add significantly to our growing understanding of how statistical thermodynamic concepts can, and cannot, be applied in active materials.

Acknowledgments: We thank Rosalind Allen, John Brady, Cristina Marchetti, and Xingbo Yang for seminal discussions. This work was funded in part by EPSRC

Grant EP/J007404. JS is supported by the Swedish Research Council (350-2012-274), RW is supported through a Postdoctoral Research Fellowship (WI 4170/1-2) from the German Research Foundation (DFG), YK is supported by the I-CORE Program of the Planning and Budgeting Committee of the Israel Science Foundation, and MEC is supported by the Royal Society. APS and JT are supported by ANR project BACTTERNS. APS, JS, MK, MEC, and JT thank the KITP at the University of California, Santa Barbara, where they were supported through National Science Foundation Grant NSF PHY11-25925.

-
- [1] M. C. Marchetti, J.-F. Joanny, S. Ramaswamy, T. B. Liverpool, J. Prost, M. Rao, and R. A. Simha, *Rev. Mod. Phys.* **85**, 1143 (2013).
- [2] J. Tailleur and M. E. Cates, *Phys. Rev. Lett.* **100**, 218103 (2008)
- [3] M. E. Cates and J. Tailleur, *Europhys. Lett.* **101**, 20010 (2013)
- [4] M. E. Cates and J. Tailleur, *Ann. Rev. Cond. Matt. Phys.*, in press; arXiv:1406.3533.
- [5] Y. Fily and M. C. Marchetti, *Phys. Rev. Lett.* **108**, 235702 (2012)
- [6] G. S. Redner, M. F. Hagan and A. Baskaran, *Phys. Rev. Lett.* **110**, 055701 (2013)
- [7] L. F. Cugliandolo, *J. Phys. A* **44**, 3001 (2011)
- [8] T. W. Lion and R. J. Allen, *Europhys. Lett.* **106**, 34003 (2014); *J. Chem. Phys.* **137**, 244911 (2014)
- [9] X. B. Yang, L. M. Manning and M. C. Marchetti, *Soft Matter* **10**, 6477 (2014)
- [10] S. C. Takatori, W. Yan and J. F. Brady, *Phys. Rev. Lett.* **113**, 028103 (2014)
- [11] R. Wittkowski, A. Tiribocchi, J. Stenhammar, R. J. Allen, D. Marenduzzo and M. E. Cates, *Nature Commun.* **5**, 4351 (2014)
- [12] F. Ginot, I. Theurkauff, D. Levis, C. Ybert, L. Bocquet, L. Berthier, C. Cotton-Bizonne, *Phys. Rev. X*, in press, arXiv:1411.7175
- [13] S. A. Mallory, A. Saric, C. Valeriani, A. Cacciuto. *Phys. Rev. E* **89**, 052303 (2014)
- [14] R. Ni, M. A. Cohen-Stuart, P. G. Bolhuis, arXiv:1403.1533 (2014)
- [15] A. P. Solon, Y. Fily, A. Baskaran, M. E. Cates, Y. Kafri, M. Kardar and J. Tailleur, arXiv:1412.3952 (2014)
- [16] J. R. Henderson, *Statistical Mechanical Sum Rules*, in Fundamentals of Inhomogeneous Fluids, D. Henderson, Ed., Marcel Dekker, New York (1992)
- [17] M. P. Allen and D. J. Tildesley, *Computer Simulation of Liquids*, Oxford University Press, Oxford (1987)
- [18] M. Doi, *Soft Matter Physics*, Oxford University Press, Oxford (2013)
- [19] R. Matas-Navarro, R. Golestanian, T. B. Liverpool and S. M. Fielding, *Phys. Rev. E* **90**, 032304 (2014); A. Zoettl and H. Stark, *Phys. Rev. Lett.* **112**, 118101 (2014)
- [20] J. Stenhammar, A. Tiribocchi, R. J. Allen, D. Marenduzzo and M. E. Cates, *Phys. Rev. Lett.* **111**, 147502 (2013)
- [21] J. Stenhammar, D. Marenduzzo, R. J. Allen and M. E. Cates, *Soft Matter* **10**, 1489 (2014)
- [22] T. Speck, J. Bialké, A. M. Menzel and H. Löwen, *Phys. Rev. Lett.* **112**, 218304 (2014)
- [23] A. Wysocki, R. G. Winkler and G. Gompper, *Europhys. Lett.* **105**, 48004 (2014)
- [24] I. Buttinoni, J. Bialké, F. Kümmel, H. Löwen, C. Bechinger and T. Speck, *Phys. Rev. Lett.* **110**, 238301 (2013)
- [25] J. R. Howse, R. A. L. Jones, A. J. Ryan, T. Gough, R. Vafabakhsh and R. Golestanian, *Phys. Rev. Lett.* **99**, 048102 (2007)
- [26] J. Palacci, S. Sacanna, A. P. Stenberg, D. J. Pine and P. M. Chaikin, *Science* **339**, 936 (2013)
- [27] I. Theurkauff, C. Cottin-Bizonne, J. Palacci, C. Ybert and L. Bocquet, *Phys. Rev. Lett.* **108**, 268303 (2012)
- [28] S. Thutupalli, R. Seeman and S. Herminghaus, *New J. Phys.* **13**, 073021 (2011)
- [29] Any self-propelled entity whose motility depends on frictional contact with a support (such as human walking, cell crawling [30], vibrated granular materials [31], or colloids that move by rolling on a surface [32]) is exchanging momentum with an external reservoir (the support).
- [30] E. Tjhung, D. Marenduzzo and M. E. Cates, *Proc. Nat. Acad. Sci. USA* **109**, 12381 (2012)
- [31] J. Deseigne, O. Dauchot, H. Chaté, *Phys. Rev. Lett.* **105**, 098001 (2010); V. Narayan, S. Ramaswamy, N. Menon, *Science* **317**, 105 (2007)
- [32] A. Bricard, J. B. Caussin, N. Desreumaux, O. Dauchot, and D. Bartolo, *Nature* **503**, 95 (2013)
- [33] A. P. Solon *et al.* In preparation.
- [34] Y. Fily, S. Henkes and M. C. Marchetti, *Soft Matter* **10**, 2132 (2014)
- [35] F. D. C. Farrell, J. Tailleur, D. Marenduzzo, M. C. Marchetti, *Phys. Rev. Lett.* **108**, 248101 (2012)
- [36] D. S. Dean, *J. Phys. A. Math. Gen.* **29**, L613 (1996)
- [37] We assume, without loss of generality, that translational invariance in y is maintained even if the system undergoes phase separation into two or more isotropic phases.
- [38] S. C. Takatori and J. F. Brady, arXiv:1411.5776 (2014)
- [39] Supplemental Material is available at [URL will be provided by the publisher].
- [40] The large deviation functional (LDF, or effective free energy) $\mathcal{F}[\hat{\rho}(\mathbf{r})]/(Vk_B T)$ for the fluctuating density $\hat{\rho}$ in a nonequilibrium system is defined as $-\ln(\text{Pr}[\hat{\rho}(\mathbf{r})])/V$

where Pr is the steady-state probability distribution [41]. In [6, 7], it is shown that $\int f(\hat{\rho})d^d r/(Vk_B T)$ is, within the local approximation, the LDF for a system of particles with a density-dependent swim speed $v(\rho)$.

- [41] R. S. Ellis, *Entropy, Large Deviations and Statistical Mechanics*, Springer Verlag, Berlin (1985)
- [42] An additional simulation at $\text{Pe} = 500$ gave a lower binodal value, $\rho/\rho_0 \simeq 0.08$. This may be due to the non-local gradient terms identified in [8].
- [43] C. Y. D. Lu, P. D. Olmsted and R. C. Ball, *Phys. Rev. Lett.* **84**, 642 (2000)
- [44] M. B. Miller and B. L. Bassler, *Ann. Rev. Microbiol.* **55**, 165 (2001)
- [45] M. E. Cates, *Rep. Prog. Phys.* **75**, 042601 (2012)
- [46] The following is cited in Supplemental Material [39]: S. J. Plimpton, *J. Comp. Phys.* **117**, 1 (1995);

Supplementary Material

I. PROOF OF RELATION $P_0 + P_1 = P_S$

We prove here (setting $D_t = 0$ for simplicity, and working in $d = 2$ dimensions) that the sum of the ideal pressure $P_0 = \rho v_0^2 / (2D_r)$ and the indirect interaction pressure $P_1 = v_0 I_2 / D_r$ is the swim pressure $P_S = \rho \langle \mathbf{r} \cdot \mathbf{F}^a \rangle / 2$, where the self-propulsion force $\mathbf{F}^a = v_0 \mathbf{u}$ was defined in (16) in the main text. (As in the main text, we set the particle mobility $v_0 / F^a = 1$ in this section, where $F^a \equiv \|\mathbf{F}^a\|$.) In proving the required result, we also establish that $P_S = \rho v_0 v(\rho) / (2D_r)$, and hence that $v(\rho) = v_0 + 2I_2 / \rho$.

We start from (see (6) in the main text)

$$I_2 = \int F_x(\mathbf{r}' - \mathbf{r}) \langle \hat{\rho}(\mathbf{r}') \hat{\mathcal{P}}(\mathbf{r}) \rangle d^2 r' \quad (17)$$

and use¹

$$\hat{\rho}(\mathbf{r}) = \sum_i \delta(\mathbf{r} - \mathbf{r}_i), \quad (18)$$

$$\hat{\mathcal{P}}(\mathbf{r}) = \sum_i \cos(\theta_i) \delta(\mathbf{r} - \mathbf{r}_i) \quad (19)$$

as well as the fact that the system is isotropic to rewrite (17) in the form

$$I_2 = \frac{1}{L_x L_y} \left\langle \sum_{i,j \neq i} F_x(\mathbf{r}_j - \mathbf{r}_i) \cos(\theta_i) \right\rangle. \quad (20)$$

We now take the thermodynamic limit: $L_x = L_y = \sqrt{A} \rightarrow \infty$. Since the system is isotropic, a similar expression can be written interchanging x and y , noting that $\cos(\theta_i) = \mathbf{u}_i \cdot \mathbf{e}_x$ with $\mathbf{u}_i = (\cos(\theta_i), \sin(\theta_i))$ and $\mathbf{e}_x = (1, 0)$. Averaging the two results gives

$$P_1 = \frac{v_0}{2D_r A} \left\langle \sum_{i,j \neq i} \mathbf{F}(\mathbf{r}_j - \mathbf{r}_i) \cdot \mathbf{u}_i \right\rangle. \quad (21)$$

We may also write, using the fact that $\mathbf{u} \cdot \mathbf{u} = 1$,

$$P_0 = \frac{\rho v_0^2}{2D_r} = \frac{v_0}{2D_r A} \sum_i v_0 \langle \mathbf{u}_i \cdot \mathbf{u}_i \rangle. \quad (22)$$

Hence, we obtain

$$P_0 + P_1 = \frac{v_0}{2D_r A} \left\langle \sum_i \left(v_0 \mathbf{u}_i + \sum_{j \neq i} \mathbf{F}(\mathbf{r}_j - \mathbf{r}_i) \right) \cdot \mathbf{u}_i \right\rangle. \quad (23)$$

From the Langevin equation (1) in the main text, applied in bulk where the wall force F_w vanishes, and setting

$D_t = 0$, we have that the term $v_0 \mathbf{u}_i + \sum_{j \neq i} \mathbf{F}(\mathbf{r}_j - \mathbf{r}_i)$ in (23) is the instantaneous particle velocity $\dot{\mathbf{r}}_i$:

$$P_0 + P_1 = \frac{v_0}{2D_r A} \left\langle \sum_i \dot{\mathbf{r}}_i \cdot \mathbf{u}_i \right\rangle. \quad (24)$$

If we redefine $\langle \cdot \rangle$ to include an average over the particle index, this may be written

$$P_0 + P_1 = \frac{\rho v_0}{2D_r} \langle \dot{\mathbf{r}} \cdot \mathbf{u} \rangle = \frac{\rho v_0}{2D_r} v(\rho). \quad (25)$$

Here, the second equality follows from the definition of $v(\rho) \equiv \langle \dot{\mathbf{r}} \cdot \mathbf{u} \rangle$ as the average speed of a particle along its propulsive direction (in a bulk system at density ρ).

Meanwhile, P_S is defined via (16) in the main text (setting $d = 2$ there) as an equal-time average

$$P_S = \frac{\rho}{2} \langle \mathbf{r} \cdot \mathbf{F}^a \rangle = \frac{\rho v_0}{2} \langle \mathbf{r} \cdot \mathbf{u} \rangle. \quad (26)$$

We rewrite $\mathbf{r}(t) = \mathbf{r}(-\infty) + \int_{-\infty}^t \dot{\mathbf{r}}(t') dt'$, and use time stationarity and the fact that $\langle \mathbf{r}(-\infty) \cdot \mathbf{u}(t) \rangle = 0$ to obtain

$$\langle \mathbf{r}(t) \cdot \mathbf{u}(t) \rangle = \int_0^\infty \langle \dot{\mathbf{r}}(0) \cdot \mathbf{u}(t') \rangle dt'. \quad (27)$$

Next, we use the fact that the angular dynamics of \mathbf{u} are autonomous: the rotational diffusion of one particle is unaffected by the location and orientation of any other particle. Then $\dot{\mathbf{r}}(0)$ and $\mathbf{u}(t')$ are correlated, but only because each is separately correlated with $\mathbf{u}(0)$. That separability allows us to write

$$\langle \dot{\mathbf{r}}(0) \cdot \mathbf{u}(t') \rangle = \frac{1}{2\pi} \int \langle \dot{\mathbf{r}}(0) | \mathbf{u}(0) \rangle \cdot \langle \mathbf{u}(t') | \mathbf{u}(0) \rangle d\theta(0), \quad (28)$$

where the integration is over the bulk steady state orientations $\theta(0) = \arccos(u_x(0))$ with uniform probability density $1/(2\pi)$, and $\langle \mathbf{X} | \mathbf{Y} \rangle$ denotes the conditional average of \mathbf{X} given \mathbf{Y} . The first conditional average in (28) obeys

$$\langle \dot{\mathbf{r}}(0) | \mathbf{u}(0) \rangle = v(\rho) \mathbf{u}(0), \quad (29)$$

which follows from the definition of $v(\rho)$ [see (25)] and the fact that the mean velocity of a particle must point along its axis \mathbf{u} , given isotropy of the bulk system. The second conditional average in (28) is found from the autonomous rotational dynamics as

$$\langle \mathbf{u}(t') | \mathbf{u}(0) \rangle = \mathbf{u}(0) \exp(-D_r t'), \quad (30)$$

which (again given isotropy) is implied by the familiar decay of angular correlations $\langle \mathbf{u}(t') \cdot \mathbf{u}(0) \rangle = \exp(-D_r t')$. It follows from (29) and (30) that the product of the conditional averages in (28) is $v(\rho) \exp(-D_r t')$, which is independent of $\mathbf{u}(0)$ as befits an isotropic system. This gives finally, upon performing the time integral in (27),

$$\langle \mathbf{r} \cdot \mathbf{u} \rangle = \frac{v(\rho)}{D_r}, \quad (31)$$

¹ Equations (18) and (19) follow from $\hat{\psi}(\mathbf{r}, \theta) = \sum_i \delta(\mathbf{r} - \mathbf{r}_i) \delta(\theta - \theta_i)$ and the definitions of $\hat{\rho}(\mathbf{r})$ and $\hat{\mathcal{P}}(\mathbf{r})$.

thus completing the proof that P_S defined by (26) is exactly equal to $P_0 + P_1$ as given by (25). Note that (31) can also be proved directly, avoiding the use of conditional averages, by a route involving Itô calculus [1].

Having proved in (25) that (with $P_0 = \rho v_0^2 / (2D_r)$) the indirect pressure $P_1 = v_0 I_2 / D_r$ obeys

$$P_1 = \frac{\rho v_0}{2D_r} (v(\rho) - v_0), \quad (32)$$

it follows, as stated in the main text, that

$$v(\rho) = v_0 + 2I_2 / \rho. \quad (33)$$

We know from ABP simulations [2] that, except at very high densities, $v(\rho)$ has the form $v(\rho) = v_0(1 - \rho/\rho_0)$ with a constant ρ_0 , so that I_2 scales like $I_2 \propto -v_0\rho^2$.

Although we have set $D_t = 0$ when deriving these results, it is simple to establish that the only direct effect of nonzero D_t is to add a term $D_t\rho$ to P_0 [1]. There is also an indirect effect on P_D and P_1 because $D_t \neq 0$ alters the correlation functions appearing in I_1 and I_2 .

II. NUMERICAL METHODS

All simulation results presented in the main text are obtained for spherical particles whose centres are confined to two dimensions (the xy -plane) and whose propulsion directions \mathbf{u} are constrained to lie in this plane. These particles interact pairwise through a repulsive Weeks-Chandler-Andersen potential:

$$U(r) = 4\varepsilon \left[\left(\frac{\sigma}{r} \right)^{12} - \left(\frac{\sigma}{r} \right)^6 \right] + \varepsilon \quad (34)$$

with an upper cut-off at $r = 2^{1/6}\sigma$, beyond which $U = 0$. Here σ denotes the particle diameter, ε determines the interaction strength, and r is the center-to-center separation between two particles. The model was studied by solving the fully overdamped translational and rotational Langevin equations. In the current section we restore an explicit particle mobility $v_0/F^a = \beta D_t$ rather than setting this to unity. The Langevin equations then read:

$$\dot{\mathbf{r}}_i = \beta D_t (\mathbf{F}_i^{\text{tot}} + F^a \mathbf{u}_i) + \sqrt{2D_t} \boldsymbol{\eta}_i, \quad (35)$$

$$\dot{\theta}_i = \sqrt{2D_r} \xi_i, \quad (36)$$

where $\mathbf{F}_i^{\text{tot}}$ is the total conservative force acting on particle i , F^a is the constant magnitude of the self-propulsion force which acts along \mathbf{u}_i , D_t and $D_r = 3D_t/\sigma^2$ denote the translational and rotational diffusivities, respectively; $\beta = 1/(k_B T)$ is the inverse thermal energy, and $\boldsymbol{\eta}_i(t)$ and $\xi_i(t)$ are zero-mean unit-variance Gaussian white noise random variables. Simulations were carried out using the LAMMPS [3] molecular dynamics package, in a periodic box with $L_x = L_y = 150\sigma$ (corresponding to $N \approx 20000$ particles). The natural simulation units are σ , ε , and $\tau_{LJ} = \sigma^2/(\varepsilon\beta D_t)$ for length, energy, and time, respectively. In these units, a time step of 5×10^{-5} was used

throughout. As discussed in [2] and in Section III below, the Péclet number $\text{Pe} \equiv 3v_0/(D_r\sigma) = 3\beta D_t F^a/(D_r\sigma)$ was varied by adjusting D_r (and hence D_t), keeping a constant value of $F^a = 24\varepsilon/\sigma$.

The value of ρ_0 , the density where the linearly decreasing swim speed goes to zero, was determined by fitting sampled values at $\text{Pe} = 40$ (*i.e.*, just outside the phase-separated region) of $v(\rho)$ over the density range $[0, 1.15]$ to the linear function $v(\rho) = v_0(1 - \rho/\rho_0)$. The value thus obtained, $\rho_0 \approx 1.19$, was used in reporting the density data presented in the main text as a function of ρ/ρ_0 .

Binodal densities were determined from simulations by coarse-graining the local density on a grid using a weighting function $w(r) \propto \exp(-r_{\text{cut}}^2/(r_{\text{cut}}^2 - r^2))$, where r is the distance between the particle and a lattice point, and r_{cut} is a cut-off distance which was taken to be slightly larger than the lattice spacing. The local densities thus obtained were binned and plotted as a probability distribution function, where the maxima of the two density peaks were taken to represent the coexistence densities.

III. SEMI-EMPIRICAL EQUATION OF STATE

We now revert to our convention that the particle mobility is unity, and rewrite Eq. (14) of the main text as

$$P_S = \left(\frac{1}{\text{Pe}} + \frac{v(\rho, \text{Pe})}{6v_0} \text{Pe} \right) \sigma \rho v_0. \quad (37)$$

Our semi-empirical equation drops the $1/\text{Pe}$ term (which comes from passive translational diffusion) and assumes that the Pe -dependence in $v(\rho, \text{Pe})$, which arises from Pe -dependence in the bulk correlators, is negligible. For $v(\rho)$ we use the fitted linear function for $v(\rho)$ described above, with the further assumption that $v = P_S = 0$ for $\rho > \rho_0$ in order to prevent negative swim speeds (see black curve in Fig. 1 of the main text). With these assumptions (which imply that ρ_0 is itself Pe -independent), the swim pressure scales as $P_S = \sigma \rho v_0 \mathcal{G}(\rho/\rho_0) \text{Pe}$ with the function $\mathcal{G}(\rho/\rho_0) = v(\rho)/(6v_0)$. This ansatz is confirmed numerically by comparing datasets with two different Pe in Fig. 1 of the main text.

In the main text we also state the scaling hypothesis

$$P_D \equiv \sigma \rho v_0 \mathcal{S}(\rho/\rho_0, \text{Pe}) = \sigma \rho v_0 \mathcal{S}(\rho/\rho_0), \quad (38)$$

The first identity defines a reduced direct pressure \mathcal{S} ; the second equality once again requires that Pe has no direct effect on the correlators (which would enter both through the shape of the function \mathcal{S} and through ρ_0 itself). Again this is confirmed by comparing P_D for two Pe values in Fig. 1 of the main text. Since we choose to vary Pe at fixed v_0 , a single P_D function then describes all our simulations; we fit this as $P_D(\rho) = \alpha(1 - \exp(-\gamma\rho))$, with α and γ fitting parameters. Note that P_D is the pressure measured from averaging Eq. (10) of the main text over Λ (see red curve in Fig. 1 of the main text) which is

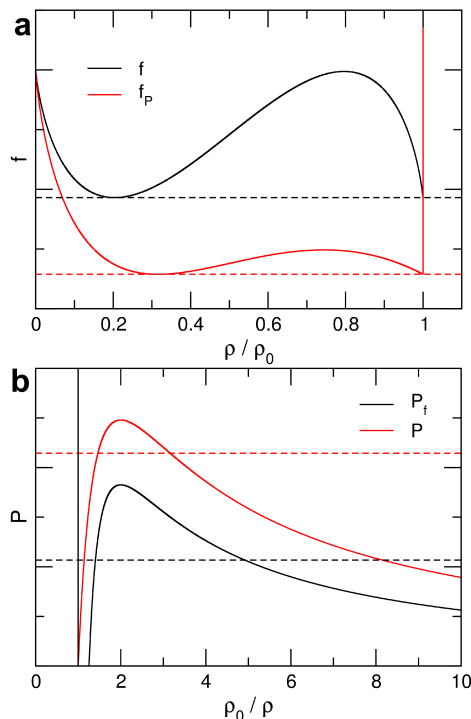


Figure 3. (a) Upper curve: CTC (dashed) on f (solid) based on (40). Lower curve: CTC (dashed) on f_P (solid) based on (43). In each case a linear term has been subtracted to make the common tangent horizontal. (b) Upper curve: MC (dashed) on the mechanical pressure $P = P_S + P_D$ (solid) based on (41). Lower curve: MC (dashed) on the pressure P_f (solid) based on (42). The curves in (a) and (b) are rescaled/displaced vertically for improved visibility.

mathematically equivalent to using the standard virial relation for pairwise additive forces [4, 5].

The above scaling forms (37) and (38) assume that, once pressures are non-dimensionalized by a factor $\sigma\rho v_0$ (recalling that the mobility is unity), there can be no further dependence on v_0 except via the dimensionless combination Pe . This is true for hard particles, but could fail for softened interactions as actually used in our simulations: in particular, at large v_0 the effective diameter of the particles seen in collisions will be less than σ ; see [2]. Accordingly the best route for testing the scalings with Pe is to vary this at fixed v_0 , as we do here.

IV. CONSTRUCTIONS OF THE BINODALS

As defined in the main text, we consider four routes (in two equivalent pairs) to calculate binodal densities in the high- Pe limit. We use ‘thermodynamic’ routes (via f, P_f) and ‘mechanical’ routes (via P, f_P), relying on the Maxwell equal-area construction (MC) and common tangent construction (CTC) as appropriate.

Method 1 starts from the effective free energy of [6, 7]

$$\tilde{f}(\rho) = k_B T \left(\rho(\ln \rho - 1) + \int_0^\rho \ln v(u) du \right), \quad (39)$$

where for ABPs $v = v_0(1 - \rho/\rho_0)$. This we supplement by a hard-core cutoff at $\rho = \rho_0$; hence f obeys

$$f = \tilde{f} \quad \text{for } \rho \leq \rho_0, \quad \text{else } f = +\infty. \quad (40)$$

The CTC is then performed on f (see Fig. 3a). Method 2 starts from the mechanical pressure $P = P_S + P_D$, representing P_D as a hard-core cutoff: $P_D = 0$ for $\rho \leq \rho_0$ and $P_D = +\infty$ for $\rho > \rho_0$. P therefore obeys

$$P = \frac{\rho v_0^2}{2D_r} (1 - \rho/\rho_0) \quad \text{for } \rho \leq \rho_0, \quad \text{else } P = +\infty. \quad (41)$$

The MC is then applied to P (see Fig. 3b). Method 3 constructs the thermodynamic pressure $P_f = \rho f' - \rho$ from f , that is

$$P_f = \rho \tilde{f}' - \tilde{f} \quad \text{for } \rho \leq \rho_0, \quad \text{else } P_f = +\infty \quad (42)$$

and then applies the MC to P_f . By mathematical necessity, this gives the same binodals as Method 1 (see Fig. 3b). Method 4 constructs a different effective free energy f_P such that $P = \rho f'_P - f_P$. The result is

$$f_P = \frac{\rho v_0^2}{2D_r} \left[\rho(\ln \rho - 1) - \frac{\rho^2}{\rho_0} \right] \quad \text{for } \rho \leq \rho_0, \quad (43)$$

$$\text{else } f_P = +\infty$$

from which binodals are found by the CTC on f_P . By mathematical necessity, this gives the same binodals as Method 2 (see Fig. 3a).

As is clear from Fig. 3, Method 1 (or 3) based on f (or P_f) gives different binodals from Method 2 (or 4) based on P (or f_P). These calculations all use the sharp cut-off approximation and hence the resulting binodals refer to the asymptotic limit of high Pe only. In this limit, Method 1 (or 3) is clearly more accurate than Method 2 (or 4) (see Fig. 2 of the main text).

However, we do not know how to generalize Method 1 (or 3) to the case of finite Pe , since we lack a theory for constructing the direct interaction contributions to f or P_f . Method 2 (or 4) does generalize, allowing use of the semi-empirical expressions for P_S and P_D described above and in the main text. However, as shown there (see Fig. 2 of the main text) the results are unsatisfactory.

None of these methods allows for nonlocal contributions, which are shown in [8] to alter the common tangent construction found by Method 1. Similar nonlocal terms are also known to arise in calculations of mechanical force balance at phase coexistence in systems undergoing continuous driving, such as in shear banding [9]; they are likewise unjustifiably neglected by Method 2 (or 4). We conclude, as stated in the main text, that no adequate theory of phase equilibria in ABPs yet exists.

-
- [1] A. P. Solon *et al.* In preparation.
 - [2] J. Stenhammar, D. Marenduzzo, R. J. Allen and M. E. Cates, *Soft Matter* **10**, 1489-1499 (2014)
 - [3] S. J. Plimpton, *J. Comp. Phys.* **117**, 1-19 (1995)
 - [4] M. P. Allen and D. J. Tildesley, *Computer Simulation of Liquids*, Oxford University Press, Oxford (1987)
 - [5] M. Doi, *Soft Matter Physics*, Oxford University Press, Oxford (2013)
 - [6] J. Tailleur and M. E. Cates, *Phys. Rev. Lett.* **100**, 218103 (2008)
 - [7] M. E. Cates and J. Tailleur, *Europhys. Lett.* **101**, 20010 (2013)
 - [8] R. Wittkowski, A. Tiribocchi, J. Stenhammar, R. J. Allen, D. Marenduzzo and M. E. Cates, *Nature Commun.* **5**, 4351 (2014)
 - [9] C. Y. D. Lu, P. D. Olmsted and R. C. Ball, *Phys. Rev. Lett.* **84**, 642 (2000)